

Supporting Information

Structural and Crystallographic Information from ^{61}Ni Solid-State NMR Spectroscopy: Diamagnetic Nickel Compounds

Peter Werhun and David L. Bryce*

Department of Chemistry and Biomolecular Sciences & Centre for Catalysis Research and Innovation

University of Ottawa

10 Marie Curie Private

Ottawa, Ontario K1N 6N5

Canada

*Author to whom correspondence may be addressed.

Tel: +1-613-562-5800 ext.2018; fax: +1-613-562-5170

Email: dbryce@uottawa.ca

Table S1: Probe information for the experiments and magnetic fields used in this work.

Field	Compound	Phase	Nuclide	Probe
21.1 T	Ni(cod) ₂	Solid	⁶¹ Ni	7 mm H/X low-gamma custom static probe
				4 mm H/X Bruker MAS probe
	Solid/ Solution	7 mm X low-gamma custom static probe		
	Ni(PPh ₃) ₄	Solid		7 mm X low-gamma custom static probe
			7 mm X low-gamma custom MAS probe	
	Ni[P(OPh) ₃] ₄	Solid	7 mm X low-gamma custom static probe	
			7 mm X low-gamma custom MAS probe	
		³¹ P	2.5 mm H/X Bruker MAS probe	
	Solution	⁶¹ Ni	7 mm X low-gamma custom static probe	
14.1 T	Ni(PPh ₃) ₄	Solution	¹³ C	5 mm H/C/N liquids autotuning cryoprobe
	Ni[P(OPh) ₃] ₄			
11.7 T	Ni(cod) ₂	Solid	⁶¹ Ni	7 mm X Bruker static solids probe with custom coil
9.4 T	Ni(cod) ₂	Solid/ Solution	⁶¹ Ni	7 mm H/X Bruker static solids probe
7.0 T	Ni(PPh ₃) ₄	Solution	³¹ P	5 mm H/X liquids autotuning broadband (BBOF) probe
			¹³ C	
	Ni[P(OPh) ₃] ₄		³¹ P	
	¹³ C			
4.7 T	Ni(PPh ₃) ₄	Solid	³¹ P	7 mm H/X/Y Bruker MAS probe

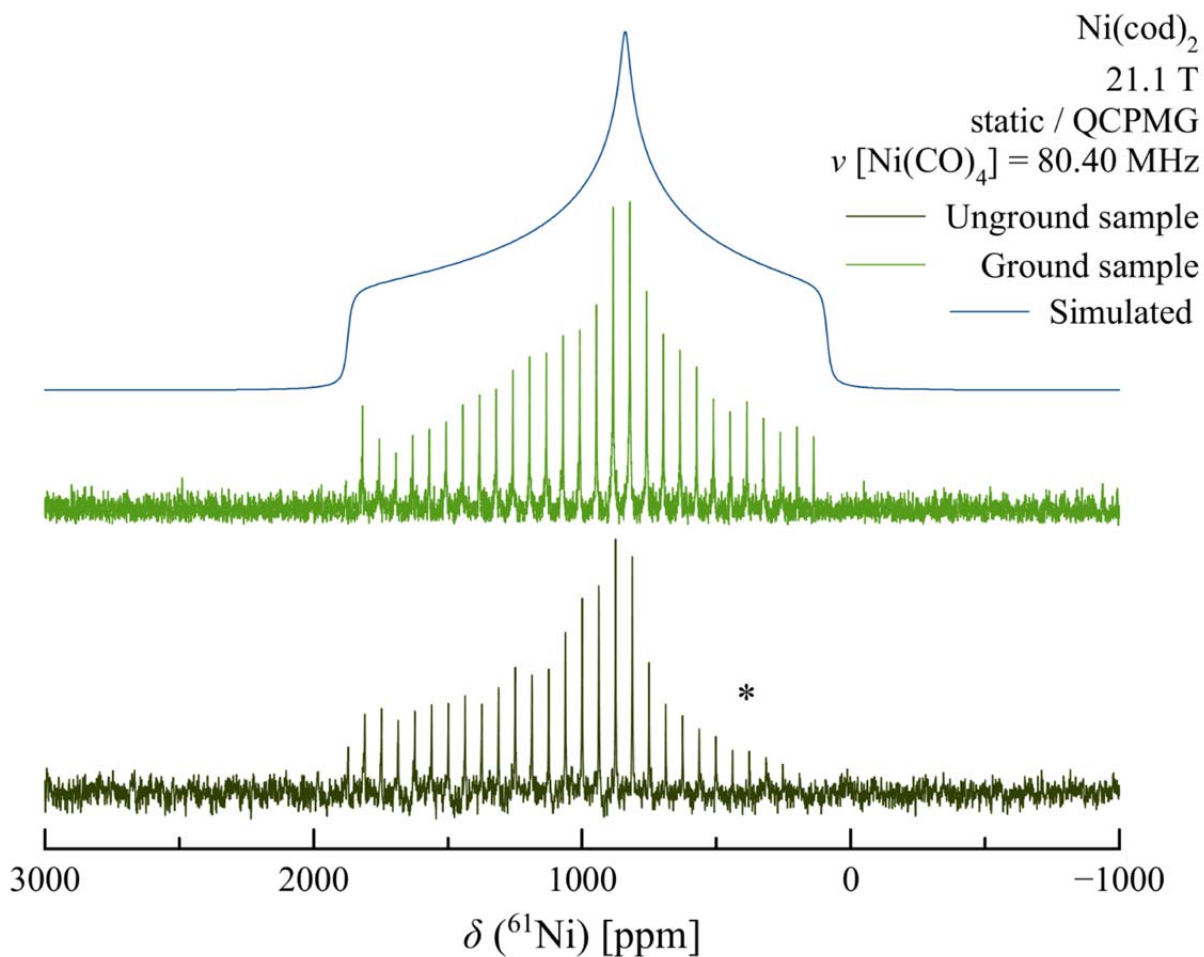


Figure S1: Experimental and simulated ^{61}Ni NMR spectra of static Ni(cod)_2 at $\nu(^1\text{H}) = 900 \text{ MHz}$. ‘*’ denotes a region of decreased intensity ascribed to preferential orientation of crystallites in the original sample tested, which consisted of platelets of olive-grey material and was not ground due to chemical sensitivity issues with the compound. The experimental details of the ground sample spectrum are provided in the main text. For the unground sample, 88k scans were acquired over 20 h with a recycle delay of 0.5 s and a spikelet separation of 5 kHz. Proton decoupling slightly increased the length of the echo train.

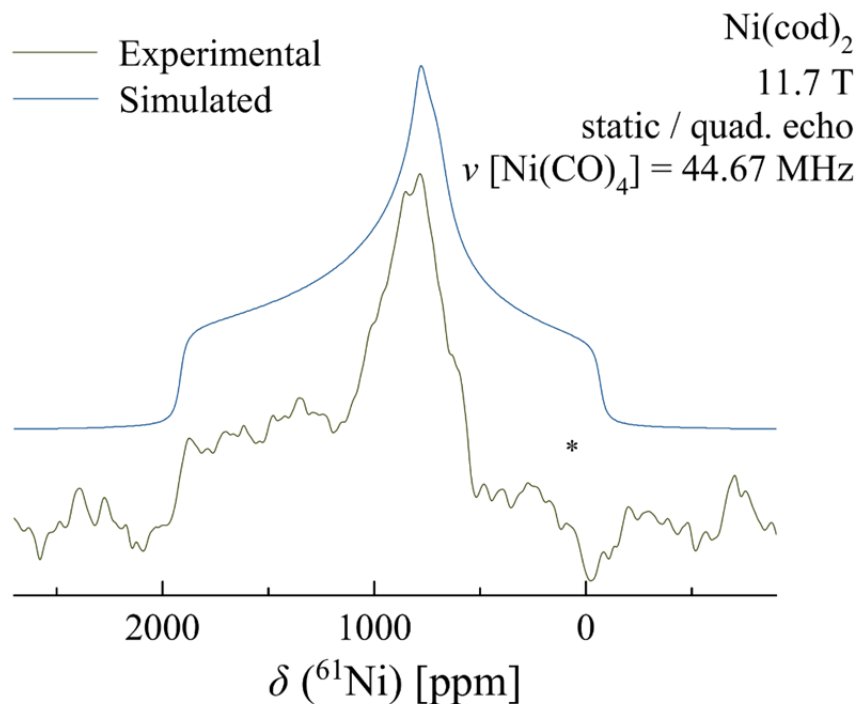


Figure S2: Experimental and simulated ^{61}Ni NMR spectra of static $\text{Ni}(\text{cod})_2$ at $\nu(^1\text{H}) = 500$ MHz. ‘*’ denotes a region of decreased intensity ascribed to preferential orientation of crystallites in the sample (see main text). The linewidth of approximately 2500 ppm corresponds to 112 kHz; the effects of pulse excitation width were determined by sampling at variable offsets and were not found to be the source of the artifact. For reasons of technical limitation a QCPMG experiment was not attempted at this field. 160k scans were acquired over 3 days using a $\pi/2$ - τ - $\pi/2$ echo with an echo time of 76 μs and recycle delay of 0.5 s.

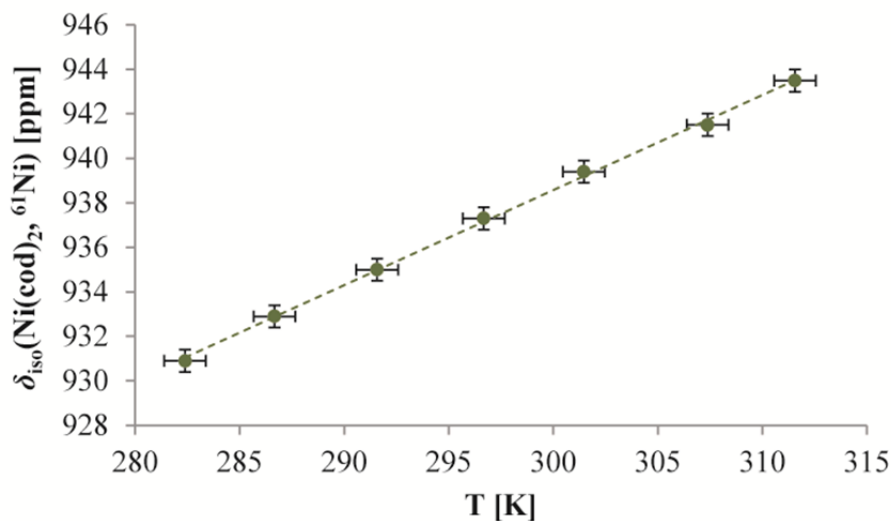


Figure S3: Temperature calibration of the ^{61}Ni δ_{iso} value of $\text{Ni}(\text{cod})_2$ saturated in C_6D_6 . The equation of the line of best fit is $\delta_{\text{iso}} = (0.4274 \pm 0.0063)T + (810.3 \pm 1.9)$, with $R^2 = 0.999$.

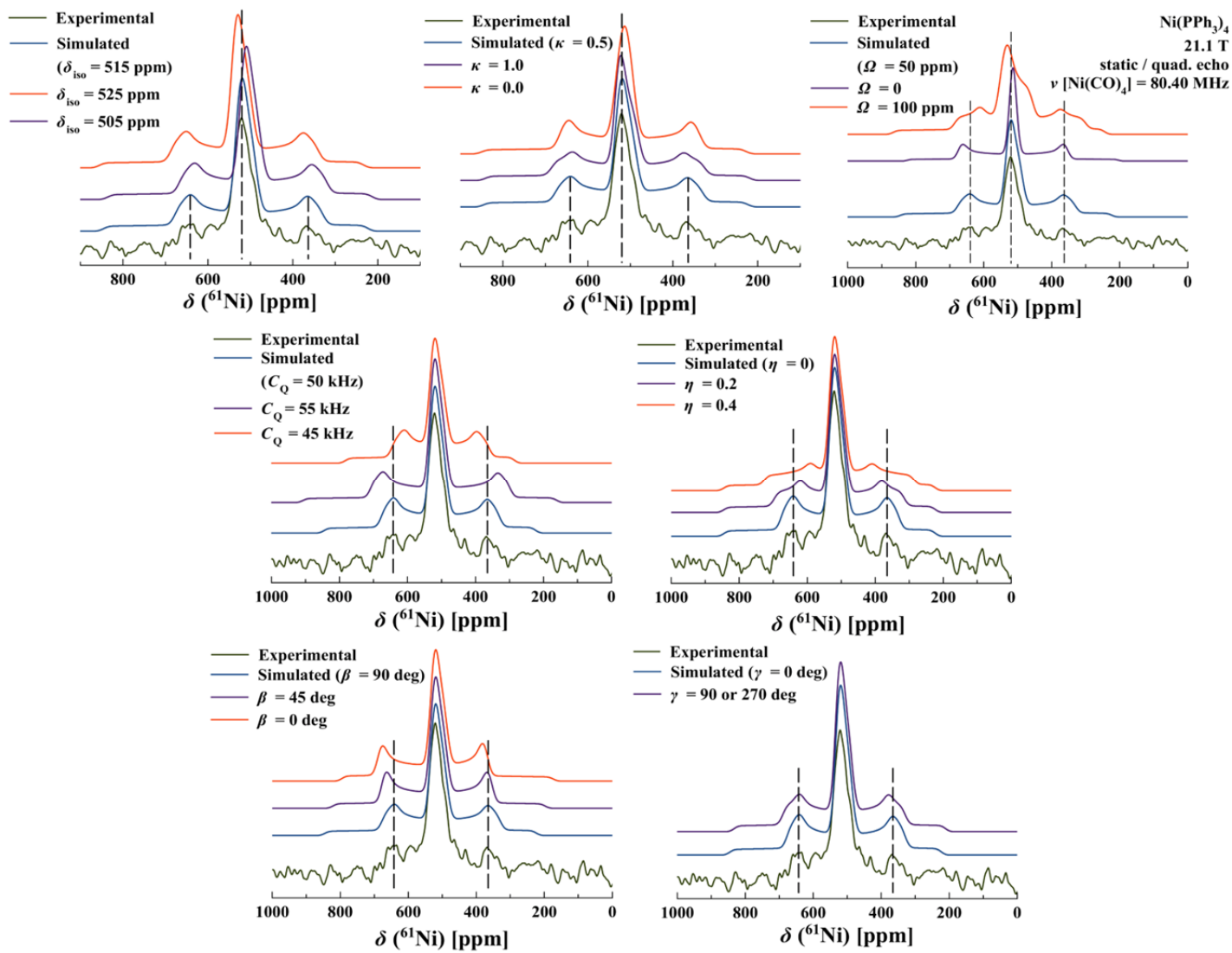


Figure S4: Demonstration of the protocol used to fit the ^{61}Ni static NMR spectrum of $\text{Ni(PPh}_3)_4$, taking advantage of the information provided by the satellite transitions.

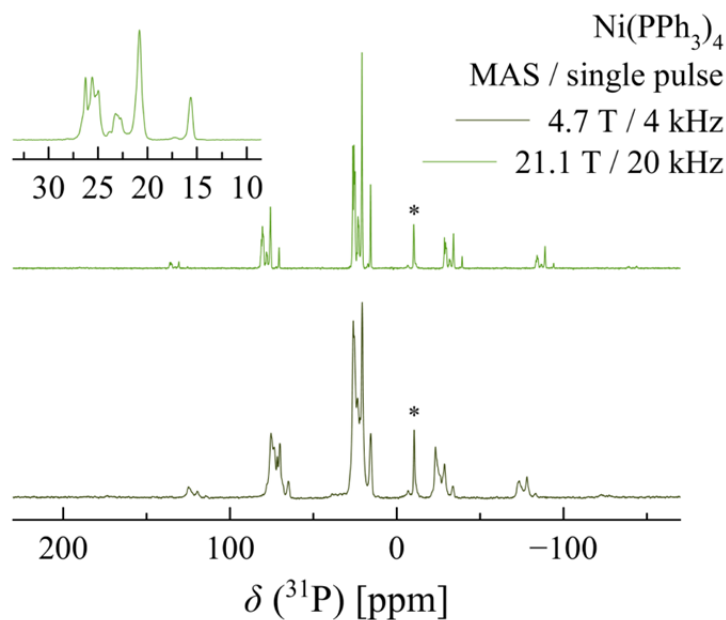


Figure S5: Experimental ^{31}P MAS NMR spectra of the sample of $\text{Ni}(\text{PPh}_3)_4$ at 4.7 and 21.1 T. Triphenylphosphine is marked with ‘*’. The other isotropic peaks are shown in the inset, with all other peaks stemming from spinning sidebands.

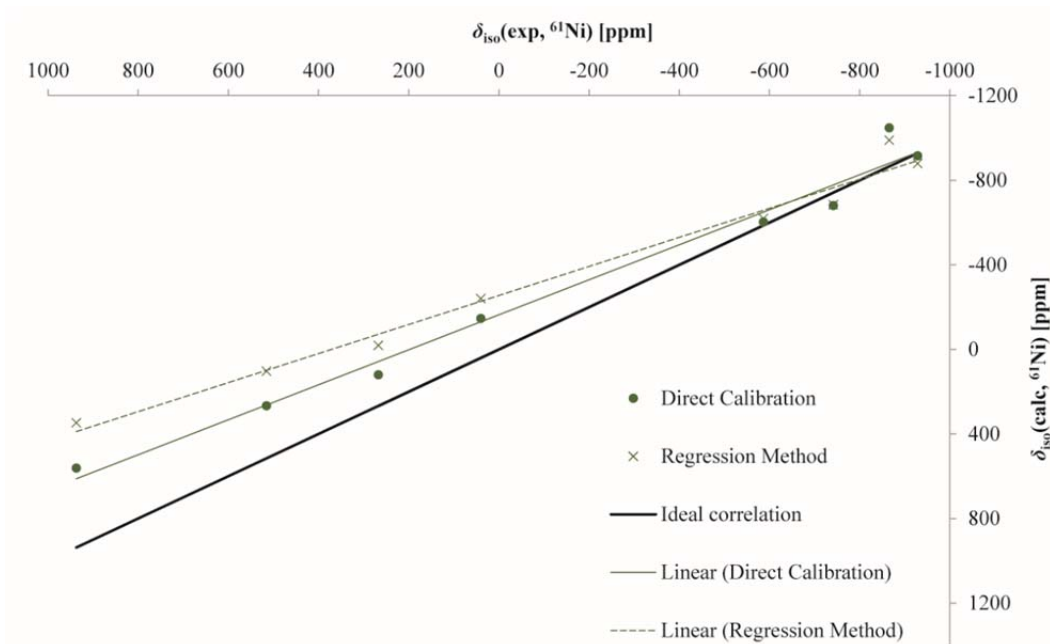


Figure S6: Correlation between experimental δ_{iso} values (see Table 3 in the main text) and δ_{iso} values obtained computationally in this work. $\text{Ni}(\text{PPh}_3)_4$ is included, using its isotropic shift as determined in the solid state. Overall, high-frequency chemical shifts appear to be systematically underestimated by the computational methods used. The equation of the line of best fit for the direct calibration is $\delta_{\text{iso}}(\text{calc}) = (0.827 \pm 0.047)\delta_{\text{iso}}(\text{exp}) - (164 \pm 32)$, with $R^2 = 0.981$ and a RMSD of 192 ppm. The equation of the line of best fit for the regression method is $\delta_{\text{iso}}(\text{calc}) = (0.687 \pm 0.039)\delta_{\text{iso}}(\text{exp}) - (254 \pm 27)$, with $R^2 = 0.981$ and a RMSD of 296 ppm.

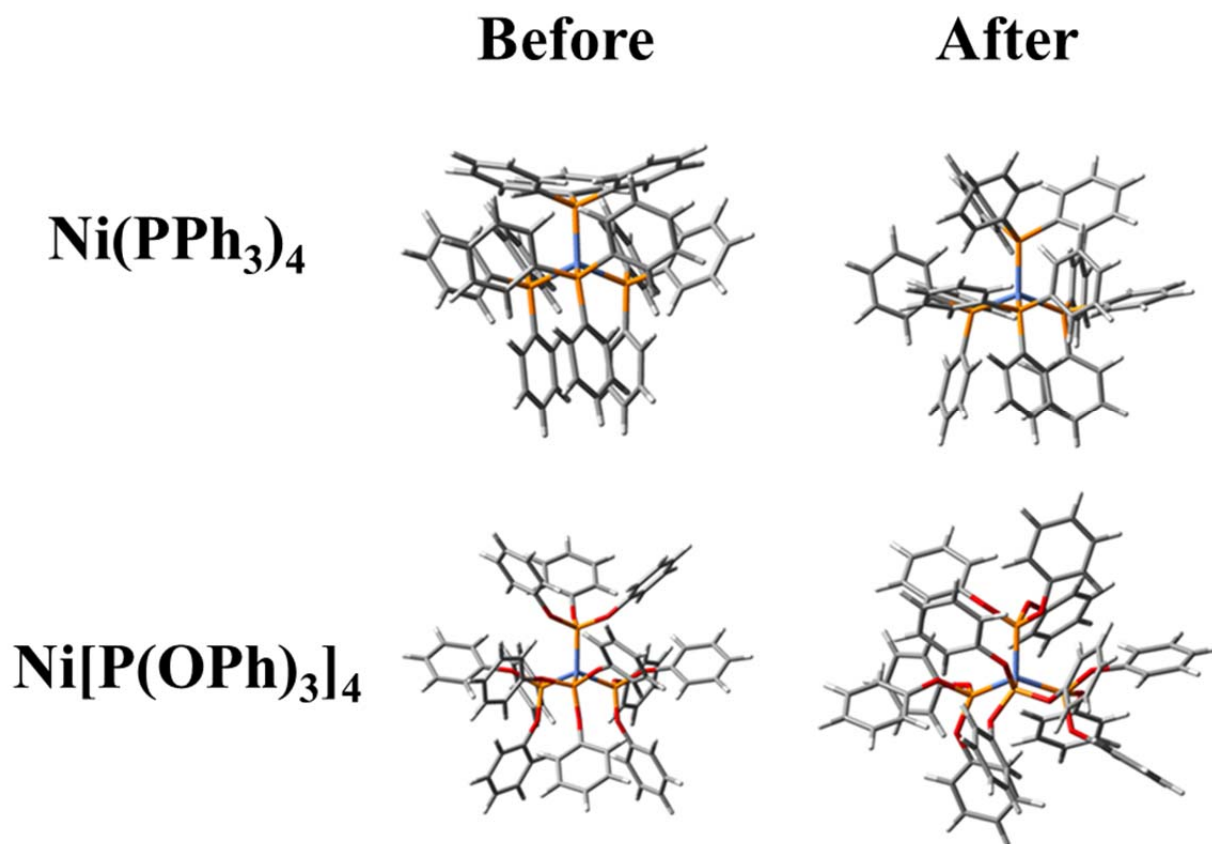


Figure S7: GaussView atomic coordinate plots of Ni(PPh₃)₄ (top) and Ni[P(OPh)₃]₄ (bottom) showing initial input structure guesses (left) and final ZORA DFT optimized structures (right). Blue denotes nickel, orange phosphorus, red oxygen, grey carbon, and white hydrogen. Note the similarity in the optimized orientations of phenyl moieties and the clear steric benefit to the inclusion of a bridging oxygen bond between the phosphorus and phenyl ring, specifically the inclusion of an extra degree of freedom in orienting the phenyl groups